

Search for gravitational waves from primordial black hole binary coalescences in the galactic halo

B. Abbott,¹² R. Abbott,¹⁵ R. Adhikari,¹³ A. Ageev,^{20,27} B. Allen,³⁹ R. Amin,³⁴ S. B. Anderson,¹² W. G. Anderson,²⁹ M. Araya,¹² H. Armandula,¹² M. Ashley,²⁸ F. Asiri,^{12,a} P. Aufmuth,³¹ C. Aulbert,¹ S. Babak,⁷ R. Balasubramanian,⁷ S. Ballmer,¹³ B. C. Barish,¹² C. Barker,¹⁴ D. Barker,¹⁴ M. Barnes,^{12,b} B. Barr,³⁵ M. A. Barton,¹² K. Bayer,¹³ R. Beausoleil,^{26,c} K. Belczynski,²³ R. Bennett,^{35,d} S. J. Berukoff,^{1,e} J. Betzwieser,¹³ B. Bhawal,¹² I. A. Bilenko,²⁰ G. Billingsley,¹² E. Black,¹² K. Blackburn,¹² L. Blackburn,¹³ B. Bland,¹⁴ B. Bochner,^{13,f} L. Bogue,¹² R. Bork,¹² S. Bose,⁴⁰ P. R. Brady,³⁹ V. B. Braginsky,²⁰ J. E. Brau,³⁷ D. A. Brown,¹² A. Bullington,²⁶ A. Bunkowski,^{2,31} A. Buonanno,^{6,g} R. Burgess,¹³ D. Busby,¹² W. E. Butler,³⁸ R. L. Byer,²⁶ L. Cadonati,¹³ G. Cagnoli,³⁵ J. B. Camp,²¹ C. A. Cantley,³⁵ L. Cardenas,¹² K. Carter,¹⁵ M. M. Casey,³⁵ J. Castiglione,³⁴ A. Chandler,¹² J. Chapsky,^{12,b} P. Charlton,^{12,h} S. Chatterji,¹³ S. Chelkowski,^{2,31} Y. Chen,⁶ V. Chickarmane,^{16,i} D. Chin,³⁶ N. Christensen,⁸ D. Churches,⁷ T. Cokelaer,⁷ C. Colacino,³³ R. Coldwell,³⁴ M. Coles,^{15,j} D. Cook,¹⁴ T. Corbitt,¹³ D. Coyne,¹² J. D. E. Creighton,³⁹ T. D. Creighton,¹² D. R. M. Crooks,³⁵ P. Csatorday,¹³ B. J. Cusack,³ C. Cutler,¹ E. D'Ambrosio,¹² K. Danzmann,^{2,31} E. Daw,^{16,k} D. DeBra,²⁶ T. Delker,^{1,34} V. Dergachev,³⁶ R. DeSalvo,¹² S. Dhurandhar,¹¹ A. Di Credico,²⁷ M. Díaz,²⁹ H. Ding,¹² R. W. P. Drever,⁴ R. J. Dupuis,³⁵ J. A. Edlund,^{12,b} P. Ehrens,¹² E. J. Elliffe,³⁵ T. Etzel,¹² M. Evans,¹² T. Evans,¹⁵ S. Fairhurst,³⁹ C. Fallnich,³¹ D. Farnham,¹² M. M. Fejer,²⁶ T. Findley,²⁵ M. Fine,¹² L. S. Finn,²⁸ K. Y. Franzen,³⁴ A. Freise,^{2,m} R. Frey,³⁷ P. Fritschel,¹³ V. V. Frolov,¹⁵ M. Fyffe,¹⁵ K. S. Ganezer,⁵ J. Garofoli,¹⁴ J. A. Giaime,¹⁶ A. Gillespie,^{12,n} K. Goda,¹³ G. González,¹⁶ S. Goßler,³¹ P. Grandclément,^{23,o} A. Grant,³⁵ C. Gray,¹⁴ A. M. Gretarsson,¹⁵ D. Grimmitt,¹² H. Grote,² S. Grunewald,¹ M. Guenther,¹⁴ E. Gustafson,^{26,p} R. Gustafson,³⁶ W. O. Hamilton,¹⁶ M. Hammond,¹⁵ J. Hanson,¹⁵ C. Hardham,²⁶ J. Harms,¹⁹ G. Harry,¹³ A. Hartunian,¹² J. Heefner,¹² Y. Hefetz,¹³ G. Heinzl,² I. S. Heng,³¹ M. Hennessy,²⁶ N. Hepler,²⁸ A. Heptonstall,³⁵ M. Heurs,³¹ M. Hewitson,² S. Hild,² N. Hindman,¹⁴ P. Hoang,¹² J. Hough,³⁵ M. Hrynevych,^{12,q} W. Hua,²⁶ M. Ito,³⁷ Y. Itoh,¹ A. Ivanov,¹² O. Jennrich,^{35,r} B. Johnson,¹⁴ W. W. Johnson,¹⁶ W. R. Johnston,²⁹ D. I. Jones,²⁸ L. Jones,²⁸ D. Jungwirth,^{12,s} V. Kalogera,²³ E. Katsavounidis,¹³ K. Kawabe,¹⁴ S. Kawamura,²² W. Kells,¹² J. Kern,^{15,t} A. Khan,¹⁵ S. Killbourn,³⁵ C. J. Killow,³⁵ C. Kim,²³ C. King,¹² P. King,¹² S. Klimenko,³⁴ S. Koranda,³⁹ K. Kötter,³¹ J. Kovalik,^{15,b} D. Kozak,¹² B. Krishnan,¹ M. Landry,¹⁴ J. Langdale,¹⁵ B. Lantz,²⁶ R. Lawrence,¹³ A. Lazzarini,¹² M. Lei,¹² I. Leonor,³⁷ K. Libbrecht,¹² A. Libson,⁸ P. Lindquist,¹² S. Liu,¹² J. Logan,^{12,u} M. Lormand,¹⁵ M. Lubinski,¹⁴ H. Lück,^{2,31} T. T. Lyons,^{12,u} B. Machenschalk,¹ M. MacInnis,¹³ M. Mageswaran,¹² K. Mailand,¹² W. Majid,^{12,b} M. Malec,^{2,31} F. Mann,¹² A. Marin,^{13,v} S. Márka,^{12,w} E. Maros,¹² J. Mason,^{12,x} K. Mason,¹³ O. Matherny,¹⁴ L. Matone,¹⁴ N. Mavalvala,¹³ R. McCarthy,¹⁴ D. E. McClelland,³ M. McHugh,¹⁸ J. W. C. McNabb,²⁸ G. Mendell,¹⁴ R. A. Mercer,³³ S. Meshkov,¹² E. Messaritaki,³⁹ C. Messenger,³³ V. P. Mitrofanov,²⁰ G. Mitselmakher,³⁴ R. Mittleman,¹³ O. Miyakawa,¹² S. Miyoki,^{12,y} S. Mohanty,²⁹ G. Moreno,¹⁴ K. Mossavi,² G. Mueller,³⁴ S. Mukherjee,²⁹ P. Murray,³⁵ J. Myers,¹⁴ S. Nagano,² T. Nash,¹² R. Nayak,¹¹ G. Newton,³⁵ F. Nocera,¹² J. S. Noel,⁴⁰ P. Nutzman,²³ T. Olson,²⁴ B. O'Reilly,¹⁵ D. J. Ottaway,¹³ A. Ottewill,^{39,z} D. Ouimette,^{12,s} H. Overmier,¹⁵ B. J. Owen,²⁸ Y. Pan,⁶ M. A. Papa,¹ V. Parameshwaraiyah,¹⁴ A. Parameswaran,¹ C. Parameswaraiyah,¹⁵ M. Pedraza,¹² S. Penn,¹⁰ M. Pitkin,³⁵ M. Plissi,³⁵ R. Prix,¹ V. Quetschke,³⁴ F. Raab,¹⁴ H. Radkins,¹⁴ R. Rahkola,³⁷ M. Rakhmanov,³⁴ S. R. Rao,¹² K. Rawlins,¹³ S. Ray-Majumder,³⁹ V. Re,³³ D. Redding,^{12,b} M. W. Regehr,^{12,b} T. Regimbau,⁷ S. Reid,³⁵ K. T. Reilly,¹² K. Reithmaier,¹² D. H. Reitze,³⁴ S. Richman,^{13,aa} R. Riesen,¹⁵ K. Riles,³⁶ B. Rivera,¹⁴ A. Rizzi,^{15,ab} D. I. Robertson,³⁵ N. A. Robertson,^{26,35} L. Robison,¹² S. Roddy,¹⁵ J. Rollins,¹³ J. D. Romano,⁷ J. Romie,¹² H. Rong,^{34,n} D. Rose,¹² E. Rotthoff,²⁸ S. Rowan,³⁵ A. Rüdiger,² P. Russell,¹² K. Ryan,¹⁴ I. Salzman,¹² V. Sandberg,¹⁴ G. H. Sanders,^{12,ac} V. Sannibale,¹² B. Sathyaprakash,⁷ P. R. Saulson,²⁷ R. Savage,¹⁴ A. Sazonov,³⁴ R. Schilling,² K. Schlaufman,²⁸ V. Schmidt,^{12,ad} R. Schnabel,¹⁹ R. Schofield,³⁷ B. F. Schutz,^{1,7} P. Schwinberg,¹⁴ S. M. Scott,³ S. E. Seader,⁴⁰ A. C. Searle,³ B. Sears,¹² S. Seel,¹² F. Seifert,¹⁹ A. S. Sengupta,¹¹ C. A. Shapiro,^{28,ae} P. Shawhan,¹² D. H. Shoemaker,¹³ Q. Z. Shu,^{34,af} A. Sibley,¹⁵ X. Siemens,³⁹ L. Sievers,^{12,b} D. Sigg,¹⁴ A. M. Sintes,^{1,32} J. R. Smith,² M. Smith,¹³ M. R. Smith,¹² P. H. Sneddon,³⁵ R. Spero,^{12,b} G. Stapfer,¹⁵ D. Steussy,⁸ K. A. Strain,³⁵ D. Strom,³⁷ A. Stuver,³⁸ T. Summerscales,²⁸ M. C. Sumner,¹² P. J. Sutton,¹² J. Sylvestre,^{12,ag} A. Takamori,¹² D. B. Tanner,³⁴ H. Tariq,¹² I. Taylor,⁷ R. Taylor,³⁵ R. Taylor,¹² K. A. Thorne,²⁸ K. S. Thorne,⁶ M. Tibbits,²⁸ S. Tilav,^{12,ah} M. Tinto,^{4,b} K. V. Tokmakov,²⁰ C. Torres,²⁹ C. Torrie,¹² G. Traylor,¹⁵ W. Tyler,¹² D. Ugolini,³⁰ C. Ungarelli,³³ M. Vallisneri,^{6,ai} M. van Putten,¹³ S. Vass,¹² A. Vecchio,³³ J. Veitch,³⁵ C. Vorvick,¹⁴ S. P. Vyachanin,²⁰ L. Wallace,¹² H. Walther,¹⁹ H. Ward,³⁵ B. Ware,^{12,b} K. Watts,¹⁵

D. Webber,¹² A. Weidner,¹⁹ U. Weiland,³¹ A. Weinstein,¹² R. Weiss,¹³ H. Welling,³¹ L. Wen,¹² S. Wen,¹⁶
 J. T. Whelan,¹⁸ S. E. Whitcomb,¹² B. F. Whiting,³⁴ S. Wily,⁵ C. Wilkinson,¹⁴ P. A. Willems,¹²
 P. R. Williams,^{1,aj} R. Williams,⁴ B. Willke,³¹ A. Wilson,¹² B. J. Winjum,^{28,e} W. Winkler,² S. Wise,³⁴
 A. G. Wiseman,³⁹ G. Woan,³⁵ D. Woods,¹ R. Wooley,¹⁵ J. Worden,¹⁴ W. Wu,³⁴ I. Yakushin,¹⁵
 H. Yamamoto,¹² S. Yoshida,²⁵ K. D. Zaleski,²⁸ M. Zanolin,¹³ I. Zawischa,^{31,ak} L. Zhang,¹¹ R. Zhu,¹ N. Zotov,¹⁷
 M. Zucker,¹⁵ and J. Zweizig¹²

(LIGO Scientific Collaboration)

¹*Albert-Einstein-Institut, Max-Planck-Institut für Gravitationsphysik, D-14476 Golm, Germany*

²*Albert-Einstein-Institut, Max-Planck-Institut für Gravitationsphysik, D-30167 Hannover, Germany*

³*Australian National University, Canberra, 0200, Australia*

⁴*California Institute of Technology, Pasadena, California 91125, USA*

⁵*California State University Dominguez Hills, Carson, California 90747, USA*

⁶*Caltech-CaRT, Pasadena, California 91125, USA*

⁷*Cardiff University, Cardiff, CF2 3YB, United Kingdom*

⁸*Carleton College, Northfield, Minnesota 55057, USA*

⁹*Fermi National Accelerator Laboratory, Batavia, Illinois 60510, USA*

¹⁰*Hobart and William Smith Colleges, Geneva, New York 14456, USA*

¹¹*Inter-University Centre for Astronomy and Astrophysics, Pune-411007, India*

¹²*LIGO—California Institute of Technology, Pasadena, California 91125, USA*

¹³*LIGO—Massachusetts Institute of Technology, Cambridge, Massachusetts 02139, USA*

¹⁴*LIGO Hanford Observatory, Richland, Washington 99352, USA*

¹⁵*LIGO Livingston Observatory, Livingston, Louisiana 70754, USA*

¹⁶*Louisiana State University, Baton Rouge, Louisiana 70803, USA*

¹⁷*Louisiana Tech University, Ruston, Louisiana 71272, USA*

¹⁸*Loyola University, New Orleans, Louisiana 70118, USA*

¹⁹*Max Planck Institut für Quantenoptik, D-85748, Garching, Germany*

²⁰*Moscow State University, Moscow, 119992, Russia*

²¹*NASA/Goddard Space Flight Center, Greenbelt, Maryland 20771, USA*

²²*National Astronomical Observatory of Japan, Tokyo 181-8588, Japan*

²³*Northwestern University, Evanston, Illinois 60208, USA*

²⁴*Salish Kootenai College, Pablo, Montana 59855, USA*

²⁵*Southeastern Louisiana University, Hammond, Louisiana 70402, USA*

²⁶*Stanford University, Stanford, California 94305, USA*

²⁷*Syracuse University, Syracuse, New York 13244, USA*

²⁸*The Pennsylvania State University, University Park, Pennsylvania 16802, USA*

²⁹*The University of Texas at Brownsville and Texas Southmost College, Brownsville, Texas 78520, USA*

³⁰*Trinity University, San Antonio, Texas 78212, USA*

³¹*Universität Hannover, D-30167 Hannover, Germany*

³²*Universitat de les Illes Balears, E-07122 Palma de Mallorca, Spain*

³³*University of Birmingham, Birmingham, B15 2TT, United Kingdom*

³⁴*University of Florida, Gainesville, Florida 32611, USA*

³⁵*University of Glasgow, Glasgow, G12 8QQ, United Kingdom*

³⁶*University of Michigan, Ann Arbor, Michigan 48109, USA*

³⁷*University of Oregon, Eugene, Oregon 97403, USA*

³⁸*University of Rochester, Rochester, New York 14627, USA*

³⁹*University of Wisconsin—Milwaukee, Milwaukee, Wisconsin 53201, USA*

⁴⁰*Washington State University, Pullman, Washington 99164, USA*

(Received 30 May 2005; published 25 October 2005)

We use data from the second science run of the LIGO gravitational-wave detectors to search for the gravitational waves from primordial black hole binary coalescence with component masses in the range $0.2\text{--}1.0M_{\odot}$. The analysis requires a signal to be found in the data from both LIGO observatories, according to a set of coincidence criteria. No inspiral signals were found. Assuming a spherical halo with core radius 5 kpc extending to 50 kpc containing nonspinning black holes with masses in the range $0.2\text{--}1.0M_{\odot}$, we place an observational upper limit on the rate of primordial black hole coalescence of 63

per year per Milky Way halo (MWH) with 90% confidence.

DOI: [10.1103/PhysRevD.72.082002](https://doi.org/10.1103/PhysRevD.72.082002)

PACS numbers: 95.85.Sz, 04.80.Nn, 07.05.Kf, 95.35.+d

Gravitational waves from binary inspiral are among the most promising sources for the first generation of gravitational-wave interferometers. Data from the first and second LIGO science runs have been searched for binary neutron star coalescence with component masses in the range $1\text{--}3M_{\odot}$ [1,2], and a search for binary black holes with component masses $>3M_{\odot}$ is underway [3]. Here we consider binaries with component masses in the range $0.2\text{--}1M_{\odot}$. Such binaries must contain a pair of black holes in order to be detectable by LIGO. Binaries composed of low mass stellar remnants, such as white dwarfs, will coalesce before the gravitational waves from inspiral reach a high enough frequency to be detected by ground based interferometers [4]. Black holes with masses $<1M_{\odot}$ are assumed to be primordial black holes (PBHs) since

there is no known mechanism that can produce subsolar mass black holes as a product of stellar evolution.

There is evidence from gravitational microlensing surveys of the Large Magellanic Cloud (LMC) that $\sim 20\%$ of the galactic halo is composed of massive compact halo objects (MACHOs) with masses $0.15\text{--}0.9M_{\odot}$ [5]. At present the explanation of the observed excess of microlensing events is controversial. Self lensing of stars in the LMC cannot account for all the observed microlensing events [6] and there are a number of potential problems with all the events being due to white dwarfs in the halo [7,8]. The nature of the majority of observed lenses is unknown [9] and PBHs with masses $\sim 0.5M_{\odot}$ have been proposed as possible MACHO candidates [10–12]. If the MACHOs are PBHs, it will be very difficult to determine this using electromagnetic observations [13]. If such PBHs formed in the early Universe, then it has been suggested that some fraction of the PBHs may exist in binaries which are coalescing today [14,15]. If a significant fraction of MACHOs are in the form of PBHs, then estimates of the rate of PBH binary coalescence suggest that it may be a factor of 100 greater than that of binary neutron stars [15,16]. If this scenario is correct, the PBH binaries are a promising source of gravitational waves and the presence of PBHs in the halos of galaxies can be confirmed by the detection of their coalescence.

In this paper we report on a search for PBH binaries in data from the second LIGO science run (S2). The data analysis techniques used are identical to those used to search for binary neutron stars in the S2 data [2], the only difference being in the choice of the search parameters. No inspiral signals were found and so we place an upper limit on the rate of PBH binary coalescence in the galactic halo. We compare this observed rate to that estimated from microlensing observations using the model of PBH binary formation proposed in [16]. Finally we comment on possible future rate limits as the LIGO detectors improve towards their design sensitivity.

Data for the second science run was taken over 59 days from February 14 to April 14, 2003. All three LIGO detectors at the two observatories were operational: a 4 km and a 2 km interferometer at the LIGO Hanford Observatory (LHO), Washington, and a 4 km interferometer at the LIGO Livingston Observatory (LLO), Louisiana. These detectors are referred to as H1, H2, and L1, respectively. During operation, feedback to the mirror positions and to the laser frequency keeps the optical cavities near resonance, so that interference in the light from the two arms recombining at the beam splitter is strongly dependent on the difference between the lengths of the two arms. A photodiode at the antisymmetric port of the detector

^aCurrently at Stanford Linear Accelerator Center.

^bCurrently at Jet Propulsion Laboratory.

^cPermanent Address: HP Laboratories.

^dCurrently at Rutherford Appleton Laboratory.

^eCurrently at University of California, Los Angeles.

^fCurrently at Hofstra University.

^gPermanent Address: GReCO, Institut d'Astrophysique de Paris (CNRS).

^hCurrently at La Trobe University, Bundoora VIC, Australia.

ⁱCurrently at Keck Graduate Institute.

^jCurrently at National Science Foundation.

^kCurrently at University of Sheffield.

^lCurrently at Ball Aerospace Corporation.

^mCurrently at European Gravitational Observatory.

ⁿCurrently at Intel Corp.

^oCurrently at University of Tours, France.

^pCurrently at Lightconnect Inc.

^qCurrently at W. M. Keck Observatory.

^rCurrently at ESA Science and Technology Center.

^sCurrently at Raytheon Corporation.

^tCurrently at NM Institute of Mining and Technology/Magdalena Ridge Observatory Interferometer.

^uCurrently at Mission Research Corporation.

^vCurrently at Harvard University.

^wPermanent Address: Columbia University.

^xCurrently at Lockheed-Martin Corporation.

^yPermanent Address: University of Tokyo, Institute for Cosmic Ray Research.

^zPermanent Address: University College Dublin.

^{aa}Currently at Research Electro-Optics Inc.

^{ab}Currently at Institute of Advanced Physics, Baton Rouge, LA.

^{ac}Currently at Thirty Meter Telescope Project at Caltech.

^{ad}Currently at European Commission, DG Research, Brussels, Belgium.

^{ae}Currently at University of Chicago.

^{af}Currently at LightBit Corporation.

^{ag}Permanent Address: IBM Canada Ltd.

^{ah}Currently at University of Delaware.

^{ai}Permanent Address: Jet Propulsion Laboratory.

^{aj}Currently at Shanghai Astronomical Observatory.

^{ak}Currently at Laser Zentrum Hannover.

senses this light, and a digitized signal is recorded at a sampling rate of 16384 Hz. This channel can then be searched for a gravitational-wave signal. More details on the detectors' instrumental configuration and performance can be found in [17,18]. In order to avoid the possibility of correlated noise sources between the H1 and H2 detectors, we only analyze data from times when the L1 detector is operational. We demand that a candidate event be coincident between the L1 and one or both of the Hanford detectors to reduce the rate of background events due to nonastrophysical sources.

We refer to [2] for a detailed description of the data analysis pipeline. Briefly, we used matched filtering with a bank of filters constructed using second order restricted post-Newtonian templates [19–21]. The bank is designed so that the loss in signal-to-noise ratio (SNR) between a putative signal and its nearest template is no more than 5% [22]. Data was filtered in 2048 s chunks and times when the SNR ρ of a template exceeded a threshold $\rho > \rho^*$ were considered candidate triggers. Noise transients in the data may yield high values of SNR, so a time-frequency χ^2 veto [23] is used to distinguish between such events and inspiral signals. The computational resources required to perform the search are proportional to the number of templates N , which scales as $N \sim m_{\min}^{-8/3}$, where m_{\min} is the smallest binary component mass in the bank. The available resources limited the template bank to binaries with component masses above $0.2M_{\odot}$. The number of templates fluctuates over the course of the run due to changing detector noise, the average value being 14178 templates in the most sensitive detector (L1). The low frequency cutoff of the search was 100 Hz due to detector noise at lower frequencies; the resulting template durations were between 4 and 56 s. We can determine the time of an inspiral to within 1 ms, so to be considered coincident, triggers must be observed within a time window $\delta t = 11$ ms between LHO and LLO (the light travel time between the observatories is 10 ms) and within $\delta t = 1$ ms between the detectors at LHO. We use the template bank from the most sensitive detector for all three detectors and demand that the mass parameters of coincident triggers are identical $\delta m = 0$. We demand that triggers in the LHO detectors pass an amplitude consistency test. No amplitude test is applied to triggers from different observatories as the different alignment of LLO and LHO (due to their different latitudes) can occasionally cause large variations in the detected signal amplitudes for astrophysical signals. Many templates may be triggered nearly simultaneously, forming clusters of triggers; the trigger with the largest SNR from each cluster is chosen for further study; triggers separated by more than 4 s are considered unique.

The sensitivity of the detectors is measured by determining the maximum distance to which the detector is sensitive to the inspiral of a pair of $0.5M_{\odot}$ PBHs at SNR of 8; that is, the distance at which an *optimally oriented* binary

would produce a SNR of 8. This distance is referred to as the range of the detector. The detectors were at differing stages of progress towards design sensitivity during the S2 run and the sensitivity of each detector fluctuated over the course of the run in response to different noise sources. The average range of the detectors during S2 was 704 kpc for L1, 359 kpc for H1, and 239 kpc for H2. As we demand coincidence with the less sensitive Hanford detectors, the range of the search is limited to the neighborhood of the Milky Way, although there are times when L1 is sensitive to M31. The PBH binary search uses the triggered search pipeline described in [2] which takes advantage of coincidence and the difference in detector sensitivity to reduce computational cost. Data from the less sensitive detectors (H1 and H2) is only filtered if a trigger is observed in the most sensitive detector (L1). Since we demand $\delta m = 0$, the triggered search is functionally equivalent to filtering all three detectors with the same template bank and looking for coincidence.

We algorithmically select a subset (approximately 10%) of the data to be used as *playground* for tuning the analysis pipeline. The playground samples the entire data set so that it is representative of the S2 data and allows us to tune our data analysis pipeline without introducing statistical bias into the upper limit. The goal of tuning the pipeline is to maximize the efficiency of the pipeline to detection of gravitational waves from binary inspirals without producing an excessive rate of spurious candidate events. The false alarm rate of our search was set by the available computational resources. If a trigger exceeds the SNR threshold, then a χ^2 veto must be performed at 15 times the computational cost of a matched filter. This limits the SNR threshold to $\rho_* = 7$ in all three detectors. We tune our detection pipeline by attempting to maximize the detection efficiency of a population of signals which are added to the data and then sought. Since we are interested in PBH binaries in the halo of the Galaxy, the population we inject is distributed as a standard spherical halo with density distribution

$$\rho(r) \propto \frac{1}{r^2 + a^2} \quad (1)$$

where r is the galactocentric radius and $a = 5$ kpc is the halo core radius. The halo is truncated at $r = 50$ kpc. The component masses of the binaries are uniformly distributed between 0.1 and $1.0M_{\odot}$. Although the template bank is terminated at a lower mass of $0.2M_{\odot}$, we were able to tune the search so that it is possible to detect inspirals with component masses down to $\sim 0.15M_{\odot}$, as shown in Fig. 1. Detection efficiencies for $m_1, m_2 \geq 0.2M_{\odot}$ were found to be greater than 90%, consistent with that expected from consideration of the detector sensitivities. We investigated injected signals whose masses were inside the template parameter space but which were not recovered and found that the loss was due to unfavorable alignment of the binary with the detector antenna patterns. However, detection

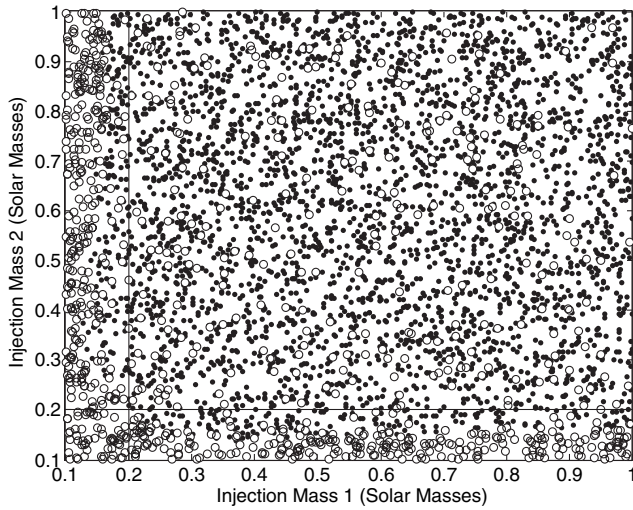


FIG. 1. 3270 inspiral signals were injected into the data using a uniform distribution in m_1 and m_2 . Each injection found by the pipeline is shown with a point and each injection missed is shown by a circle. The lines at $m_1 = m_2 = 0.2M_\odot$ show the edge of the template bank. When constructing the upper limit on the rate, we only consider injections that lie inside the region of parameter space covered by the template bank, i.e. $m_1, m_2 > 0.2M_\odot$. It can be seen that the sensitivity of the search is greatly reduced for binaries with a component of mass $< \sim 0.15$.

efficiency is uniform across the region of mass parameter space covered by the template bank. For PBH binaries, the χ^2 veto was found to be particularly powerful. No triggers were observed in the playground data.

We estimate the background rate for this search by introducing an artificial time offset $\Delta t \geq 17$ s to the triggers coming from the Livingston detector relative to the Hanford detectors. We assume the shifted triggers are uncorrelated between the observatories, however we do not time-shift the two Hanford detectors relative to each other as there may be real correlations due to environmental disturbances. The triggers which emerge at the end of the pipeline are considered a single trial representative of the output from a search if no signals are present in the data. By choosing a time shift much greater than the light travel time between the observatories, we ensure that a true gravitational-wave signal will not be coincident in the time-shifted data. If the times of background triggers are uncorrelated between observatories then the background rate is entirely due to accidental coincidences which can be estimated using the time-shift analysis. A total of 60 time shifts were analyzed to estimate the background with $\Delta t = \pm 17 + 10n$ s, where $n = 0, 1, \dots, 29$.

For a coincident trigger, the SNR observed in L1 is denoted ρ_L and the coherent SNR observed in H1 and H2 is ρ_H . The distribution of background triggers in the (ρ_L, ρ_H) plane for the PBH binary search showed a similar distribution to that of the binary neutron star search [2]; the SNR of background triggers in the Hanford detectors was

typically larger than that in the Livingston detector. In order to combine triggers from the two detectors, the SNRs of the triggers were combined as

$$\rho^2 = \rho_L^2 + \rho_H^2/4 \quad (2)$$

with any coincident triggers in the Hanford detectors combined coherently [2,24]. Figure 2 shows the sample mean and standard deviation of the expected number of accidental coincidence events per S2 observation time with combined SNR $\rho^2 > \rho_*^2$ computed from the 60 time shifts. This can be compared with the triggers observed by the search to give a visual estimate of the significance of the event candidates.

The pipeline described above was used to analyze the S2 data. After applying the data quality cuts and the L1 instrumental veto described in [2], and discarding science segments with durations less than 2048 s, a total of 375 hours of data was searched for binary coalescence. For the upper limit analysis, we only considered the nonplayground times amounting to 341 hours. (The extra 2 hours of data in this analysis compared with [2] are due to a bug fix applied to the data handling routines after completion of the analysis in [2].) The output of the pipeline is a list of candidates which are assigned a SNR according to Eq. (2). Only three candidates survive in the final sample. All these triggers lie in nonplayground data and there are no triple coincident triggers. The two loudest coincident triggers occurred when all three detectors were operating, but the SNR in H1 was too small to cross the threshold in H2, so they were accepted as coincident triggers according to our pipeline. The third coincident trigger occurred when only

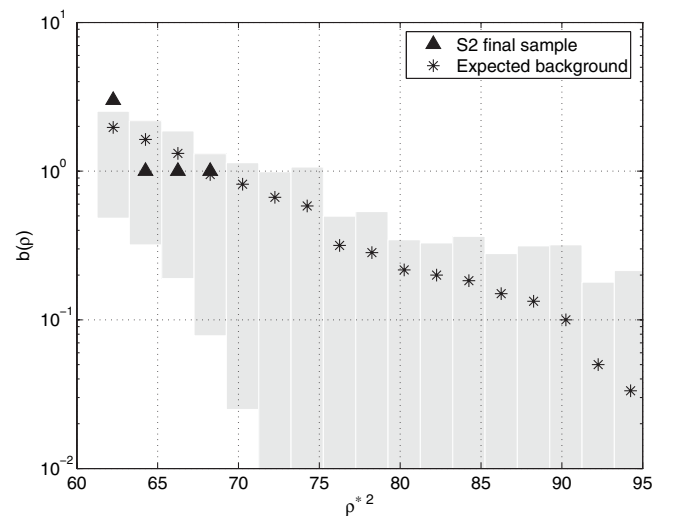


FIG. 2. The mean number of triggers per S2 observation time above combined SNR ρ^* . The stars represent the expected background based on 60 time-shift analyses. The shaded envelope indicates the standard deviation in the number of events. The triangles show the distribution of events from the final S2 sample.

the L1 and H2 detectors were operating. All three triggers had values of combined SNR very close to the threshold value of $\rho^{*2} = 61.25$.

A trigger is elevated to the status of an event candidate if the chance occurrence due to noise is small as measured by the background estimation. Event candidates are subject to further follow-up investigations beyond the level of the automated pipeline to ensure that it is not due to an instrumental or environmental disturbance. Figure 2 shows a cumulative histogram of the final coincident triggers versus ρ^2 overlaid on the expected background due to accidental coincidences. The final sample of coincident triggers appears consistent with the expected background and so we do not believe that they are due to gravitational waves. To verify this, further investigation of the three surviving triggers was performed. There is evidence of transient excess noise in the detectors at the times of all three triggers, although the origin of this noise could not be conclusively identified. The presence of transient noise, the low SNR of the triggers, and their consistency with the expected background rate due to noise leads us to believe that no gravitational-wave signals were detected by the search.

To determine an upper limit on the event rate we use the *loudest event statistic* [25] which uses the detection efficiency at the signal-to-noise ratio of the loudest trigger surviving the pipeline to determine an upper limit on the rate. The rate of PBH binary inspirals per Milky Way halo (MWH) is

$$\mathcal{R}_{90\%} = \frac{2.303 + \ln P_b}{TN_H(\rho_{\max})} \text{ yr}^{-1} \text{ MWH}^{-1} \quad (3)$$

with 90% confidence. T is the observation time of the search, N_H is the number of Milky Way halos to which the search is sensitive at the SNR threshold ρ^* of the loudest trigger ρ_{\max} , and P_b is the probability that all background triggers have SNR less than ρ_{\max} . This is a frequentist upper limit on the rate. For $\mathcal{R} > \mathcal{R}_{90\%}$, there is a probability of 90% or greater that at least one event would be observed with SNR greater than ρ^* . From the background analysis, we estimate that $P_b = 0.3 \pm 0.1$ (statistical error only); however, for this analysis we omit the background term by setting $P_b = 1$. This yields a conservative estimate of the upper limit on the rate.

During the $T = 341 \text{ h} = 0.0389 \text{ yr}$ of data used in our analysis, the largest SNR observed was $\rho_{\max}^2 = 67.4$. The number of Milky Way halos N_H was computed using a Monte-Carlo simulation in which the data was reanalyzed with simulated inspiral signals drawn from the Milky Way halo population described by Eq. (1). Although we have some sensitivity to the detection of inspirals with components below this mass, we restrict our upper limit to the region covered by the template bank $0.2 \leq m_1, m_2 \leq 1.0M_\odot$ by discarding all injections which have a component mass less than $0.2M_\odot$ when computing N_H . Figure 3

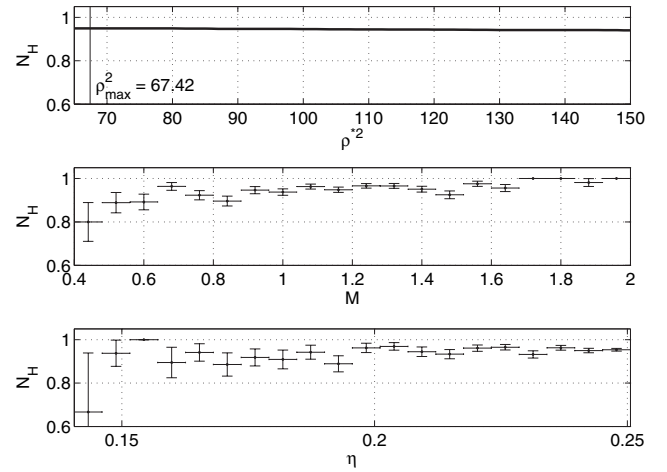


FIG. 3. The top panel shows the sensitivity in MW halos N_H of the search to the target population as a function of the loudest SNR ρ_{\max} . The largest SNR observed in this analysis was $\rho_{\max}^2 = 67.4$ meaning that the search was sensitive to a fraction $N_H = 0.95$ MWH of the halo. The middle panel shows N_H as a function of total mass $M = m_1 + m_2$ of the injected signal. The error bars show the statistical error due to the finite number of injections in the Monte-Carlo simulation. The lower panel shows N_H as a function of the symmetric mass ratio $\eta = m_1 m_2 / M^2$. We can see that the efficiency is a weak function of the total mass, as the amplitude of the inspiral signal is a function of the total mass. The efficiency of the search does not depend strongly upon η .

shows the value of N_H as a function of the loudest event ρ_{\max}^2 . At $\rho_{\max}^2 = 67.4$, we find that $N_H = 0.95$ MWH. The various contributions to the error in the measured value of detection efficiency are described in detail in [2]. In summary, the systematic errors are due to uncertainties in the instrumental response, errors in the waveform due to differences between the true inspiral signal, and the finite number of injections in the Monte-Carlo simulation. In this analysis, we neglect errors due to the spatial distribution of the PBH binaries as studies show that the upper limit is relatively insensitive to the shape of the Milky Way halo. This is because the maximum range of all three detectors is greater than 50 kpc for PBH masses $\geq 0.2M_\odot$. The systematic errors will affect the rate through the measured SNR of the loudest event. We can see that the efficiency of the search depends very weakly on the SNR of the loudest event, again due to the range of the search compared to the halo radius. The statistical errors in the Monte-Carlo analysis dominate the errors in N_H . The combined error due to waveform mismatch and the calibration uncertainty is found to be $\mathcal{O}(10^{-4})$ MWH. The effects of spin were ignored both in the population and in the waveforms used to detect inspiral signals. Estimates based on the work of Apostolatos [26] suggest that the mismatch between the signal from spinning PBHs and our templates will not significantly affect the upper limit. To be conservative, however, we place an upper limit only on

nonspinning PBHs; we will address this issue quantitatively in future analyses. Combining the errors in quadrature and assuming the downward excursion of N_H to be conservative, we obtain an observational upper limit on the rate of PBH binary coalescence with component masses $0.2\text{--}1.0M_\odot$ in the Milky Way halo to be

$$\mathcal{R}_{90\%} = 63 \text{ yr}^{-1} \text{ MWH}^{-1}. \quad (4)$$

By considering numerical simulations of three-body PBH interactions in the early Universe Ioka *et al.* [16] obtain a probability distribution for the formation rate and coalescence time of PBH binaries. This depends on the PBH mass m , which we assume to be the MACHO mass. From this distribution, we may obtain an estimate of the rate of PBH coalescence at the present time, given by

$$\mathcal{R} = 1 \times 10^{-13} \left(\frac{\mathcal{M}}{M_\odot} \right) \left(\frac{m}{M_\odot} \right)^{-(32/37)} \text{ yr}^{-1} \text{ MWH}^{-1} \quad (5)$$

where m is the MACHO mass and \mathcal{M} is the mass of the halo in MACHOs, which is obtained from microlensing observations. These measured values depend on the halo model used in the analysis of the microlensing results [27,28]. The halo model in Eq. (1) corresponds to model S of the MACHO Collaboration [27]. The microlensing observations and PBH formation models assume a δ -function mass distribution, as does the rate estimate in Eq. (5). We can see from Fig. 3 that our detection efficiency is not strongly dependent on the ratio of the binary masses η , and so we can marginalize over this parameter to obtain the rate as a function of total PBH mass M , which can be compared with the predicted rates from microlensing for different halo models. The analysis of 5.7 yrs of photometry of 11.9×10^6 stars in the LMC suggests a MACHO mass of $m = 0.79^{+0.32}_{-0.24}$ and a halo MACHO mass $\mathcal{M} = 10^{+4}_{-3} \times 10^{10} M_\odot$ for halo model S [5]. Assuming all the MACHOs are PBHs, we obtain the rate estimate $\mathcal{R} = 1.2 \times 10^{-2} \text{ yr}^{-1} \text{ MWH}^{-1}$, which is 3 orders of magnitude lower than our measured rate. Figure 4 shows a comparison of the rates predicted using the results of [5] for a standard halo (S), a large halo (B), and a small halo (F). Models B and F are power-law halos [29] and are discussed in detail in [27,28]. We note that our upper limit is not strongly dependent on the halo model as all three halos terminate before the sensitivity of our search is significantly decreased.

Finally we note that the estimated microlensing rate for the standard halo is lower than that predicted in [16], due to the tighter constraints placed on the MACHO population by the additional observation time of [5]. At design sensitivity initial LIGO will be able to see binaries containing $0.5M_\odot$ PBHs to 15 Mpc [15], when averaged over antenna

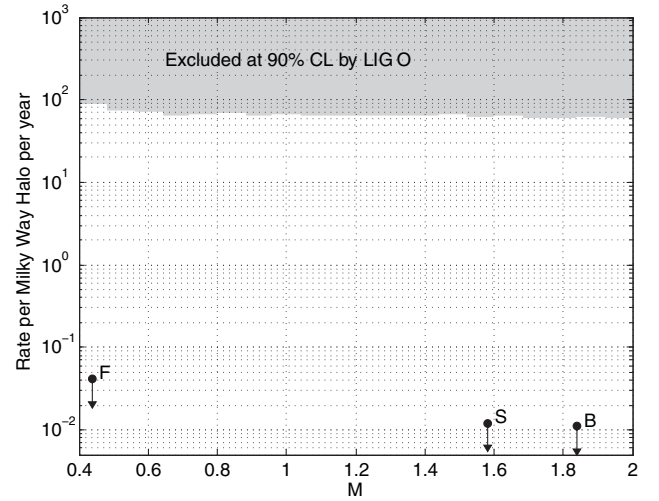


FIG. 4. The shaded region shows rates excluded at 90% confidence by the observational upper limit on PBH binary coalescence presented in this paper as a function of total mass $M = m_1 + m_2$ of the binary. The three points show the rates estimated using Eq. (5) for halo models S ($M = 1.58M_\odot$), F ($M = 0.44M_\odot$), and B ($M = 1.84M_\odot$) of [5].

pattern and binary orientation, suggesting an optimistic rate of several per year. The true rate may be much lower, or zero if no PBH binaries exist; however, the possibility of detection makes it worthwhile to extend the inspiral search used for binary neutron stars into the MACHO mass range. In the absence of detection, with 1 yr of data at design sensitivity we should be able to place limits on the rate $\mathcal{R} \sim 10^{-3} \text{ yr}^{-1} \text{ MWH}^{-1}$, assuming other galaxies have a similar MACHO halo content to our own, and hence significantly constrain the fraction of MACHOs that may be PBHs.

The authors gratefully acknowledge the support of the United States National Science Foundation for the construction and operation of the LIGO Laboratory and the Particle Physics and Astronomy Research Council of the United Kingdom, the Max-Planck-Society, and the State of Niedersachsen/Germany for support of the construction and operation of the GEO600 detector. The authors also gratefully acknowledge the support of the research by these agencies and by the Australian Research Council, the Natural Sciences and Engineering Research Council of Canada, the Council of Scientific and Industrial Research of India, the Department of Science and Technology of India, the Spanish Ministerio de Ciencia y Tecnologia, the John Simon Guggenheim Foundation, the Leverhulme Trust, the David and Lucile Packard Foundation, the Research Corporation, and the Alfred P. Sloan Foundation.

- [1] B. Abbott *et al.* (LIGO Scientific Collaboration), *Phys. Rev. D* **69**, 122001 (2004).
- [2] B. Abbott *et al.* (LIGO Scientific Collaboration), *Phys. Rev. D* **72**, 082001 (2005).
- [3] B. Abbott *et al.* (LIGO Scientific Collaboration) (to be published).
- [4] K. S. Thorne, in *Three Hundred Years of Gravitation*, edited by S. W. Hawking and W. Israel (Cambridge University Press, Cambridge, England, 1987), Chap. 9, pp. 330–458.
- [5] C. Alcock *et al.* (MACHO Collaboration), *Astrophys. J.* **542**, 281 (2000).
- [6] L. Mancini, S. C. Novati, P. Jetzer, and G. Scarpetta, *astro-ph/0405257*.
- [7] A. Spagna, D. Carollo, M. G. Lattanzi, and B. Bucciarelli, *astro-ph/0407557*.
- [8] E. Garcia-Berro, S. Torres, J. Isern, and A. Burkert, *astro-ph/0401146*.
- [9] D. P. Bennett, A. C. Becker, and A. Tomaney, *astro-ph/0501101*.
- [10] J. Yokoyama, *Astron. Astrophys.* **318**, 673 (1997).
- [11] K. Jedamzik, *Phys. Rev. D* **55**, R5871 (1997).
- [12] J. Yokoyama, *Prog. Theor. Phys. Suppl.* **136**, 338 (1999).
- [13] T. Nakamura, *Phys. Rep.* **307**, 181 (1998).
- [14] L. S. Finn, *gr-qc/9609027*.
- [15] T. Nakamura, M. Sasaki, T. Tanaka, and K. S. Thorne, *Astrophys. J.* **487**, L139 (1997).
- [16] K. Ioka, T. Chiba, T. Tanaka, and T. Nakamura, *Phys. Rev. D* **58**, 063003 (1998).
- [17] B. Abbott *et al.* (LIGO Scientific Collaboration), *Nucl. Instrum. Methods Phys. Res., Sect. A* **517**, 154 (2004).
- [18] B. Abbott *et al.* (LIGO Scientific Collaboration), *gr-qc/0501068*.
- [19] D. A. Brown, Ph.D. thesis, University of Wisconsin–Milwaukee, 2004.
- [20] B. Allen, W. G. Anderson, P. R. Brady, D. A. Brown, and J. D. E. Creighton, *gr-qc/0509116*.
- [21] LSC Algorithm Library software packages LAL and LALAPPS, the CVS tag versions *macho_2004061801* of LAL and LALAPPS were used in this analysis, <http://www.lsc-group.phys.uwm.edu/lal>.
- [22] B. J. Owen and B. S. Sathyaprakash, *Phys. Rev. D* **60**, 022002 (1999).
- [23] B. Allen, *Phys. Rev. D* **71**, 062001 (2005).
- [24] A. Pai, S. Dhurandhar, and S. Bose, *Phys. Rev. D* **64**, 042004 (2001).
- [25] P. R. Brady, J. D. E. Creighton, and A. G. Wiseman, *Classical Quantum Gravity* **21**, S1775 (2004).
- [26] T. A. Apostolatos, *Phys. Rev. D* **52**, 605 (1995).
- [27] C. Alcock *et al.* (MACHO Collaboration), *Astrophys. J.* **461**, 84 (1996).
- [28] C. Alcock, R. A. Allsman, D. Alves, T. S. Axelrod, A. C. Becker, D. P. Bennett, K. H. Cook, K. C. Freeman, K. Griest, J. Guern *et al.*, *astro-ph/9606165*.
- [29] N. W. Evans, *Mon. Not. R. Astron. Soc.* **260**, 191 (1993).